Electronic Supplementary Material (ESI) for Physical Chemistry Chemical Physics.

Supporting Information for

Enhanced magnetic anisotropy of iridium dimers on antisite defects of two-dimensional transition-metal dichalcogenides

Jun Wang,[a] *Chen Yao,*[a] *Siqi Lu,*[a,b] *Suyun Wang,*[a] *Dong Zheng,*[a,b] *Fengqi Song,*[a,b] *and Jianguo Wan,*[a,*]

[a] National Laboratory of Solid State Microstructures, Collaborative Innovation Center of Advanced Microstructures, and School of Physics, Nanjing University, Nanjing 210093, China
[b] Atomic Manufacture Institute (AMI), 211805 Nanjing, China

*Corresponding author. Jianguo Wan, E-mail: wanjg@nju.edu.cn

S1. Optimized lattice parameters of the pristine and Janus TMD nanosheets

Table S1. Optimized in-plane lattice constant of the pristine MX_2 and Janus MXY TMD nanosheets.

TMDs	a (Å)	TMDs	a (Å)
MoS_2	3.18	WS_2	3.18
$MoSe_2$	3.32	WSe_2	3.32
$MoTe_2$	3.55	WTe_2	3.55
MoSSe	3.22	WSSe	3.25
MoSTe	3.32	WSTe	3.37
MoSeTe	3.43	WSeTe	3.43

S2. The formation energies of the antisite defects from TMD monolayers

Before constructing the Ir_2@TMD-X_M system, it is necessary to indicate the formation energy of the antisite defect in our study. Here, we calculated the formation energy E_f of antisite defects X_M of TMD monolayers (see Fig. S1), which is expressed as,

$$E_f = E_{defect} - E_{pure} + \mu_M - \mu_X \quad (2\text{-}1)$$

where E_{defect} and E_{pure} present the total energies of TMD monolayer with and without antisite defects. μ_M and μ_X are the chemical potentials of metal M and chalcogen X atoms from antisite defects, respectively. The chemical potential of M and X in MX_2 should satisfy $\mu_M + 2\mu_X = \mu_M^0 + 2\mu_X^0 + \Delta H_{MX_2}$, where μ_M^0 and μ_X^0 are the chemical potential of M and X in their bulk form, respectively. ΔH_{MX_2} is the formation enthalpy of the MX_2 monolayer. Note that it is difficult to specify the exact value of the chemical potential, we can only provide ranges as $\mu_M^0 + \Delta H_{MX_2} \le \mu_M \le \mu_M^0$, $\mu_X^0 + \frac{1}{2}\Delta H_{MX_2} \le \mu_X \le \mu_X^0$ based on the M-rich and X-rich conditions. The Janus-MXY TMD (X, Y = S/Se/Te; X≠Y) monolayer is synthesized by replacing one X atom layer with a Y atom layer from the MX_2 monolayer. Based on this synthesis process, it is logical to assume that the chemical potential range is comparable to that of the MX_2 (MY_2) monolayer.

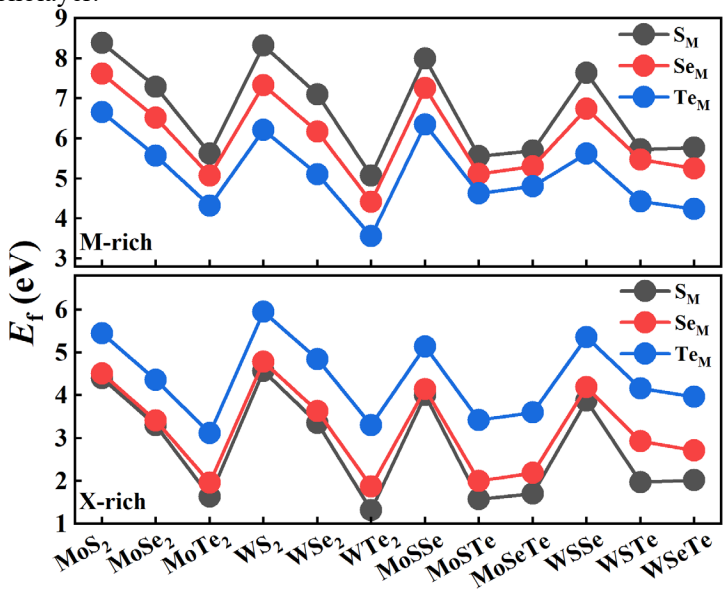

Fig. S1 The formation energies E_f of antisite defects in tradition MX_2 and Janus MXY TMD monolayers.

S3. Stability comparison of Ir_2 adsorbed on different sites of MoS_2-S_{Mo}.

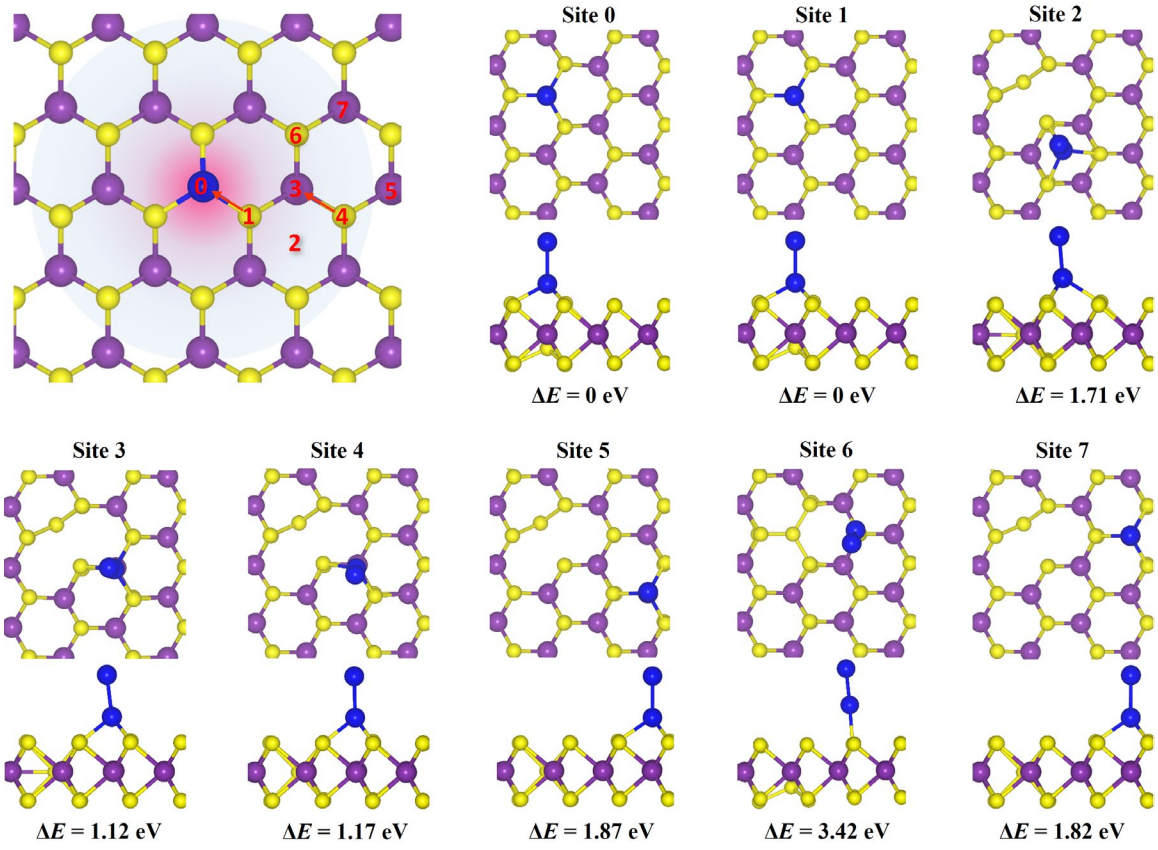

Fig. S2 Top view, side view and energy difference ΔE of Ir_2 adsorbed at the site 0-7 of MoS_2-S_{Mo} at optimal energy. Here, $\Delta E = E_{tot}^{n} - E_{tot}^{0}$, where E_{tot}^{n} and E_{tot}^{0} present the total energy of Ir_2@MoS_2-S_{Mo} at the site n (n = 1-7) and site 0, respectively.

S4. The average electrostatic potential difference of Janus TMDs with antisite defects.

Table S2. The average electrostatic potential difference ΔV (eV) of Janus TMDs with antisite defects.

TMDs	S_{Mo}	Se_{Mo}	Te_{Mo}	TMDs	S_W	Se_W	Te_W
MoSSe(↑)	0.560	0.725	0.710	WSSe(↑)	0.809	0.711	0.681
MoSSe(↓)	-0.560	-0.725	-0.710	WSSe(↓)	-0.809	-0.711	-0.681
MoSTe(↑)	1.276	1.276	1.338	WSTe(↑)	1.219	1.416	1.303
MoSTe(↓)	-1.276	-1.276	-1.338	WSTe(↓)	-1.219	-1.416	-1.303
MoSeTe(↑)	0.566	0.563	0.689	WSeTe(↑)	0.785	0.661	0.663
MoSeTe(↓)	-0.566	-0.563	-0.689	WSeTe(↓)	-0.785	-0.661	-0.663

S5. Optimized structural parameters of Ir_2@TMD-X_M nanosheets.

Table S3. Binding energies E_b (eV), included angles θ (°), degrees of tilt ρ (%), distances d (Å), Bader charges ΔQ (e) of 54 Ir_2@TMD-X_M structures.

TMDs	Defect	E_b	θ	ρ	d_{Ir^A}	d_{Ir^B}	$d_{Ir^A-Ir^B}$	d_{Ir^A-def}	ΔQ	ΔQ_{Ir^A}	ΔQ_{Ir^B}
MoS_2	S_{Mo}	-4.84	0.51	0.89	3.46	1.19	2.28	3.52	-0.221	0.144	-0.365
	Se_{Mo}	-4.25	0.51	0.89	3.47	1.19	2.28	3.46	-0.224	0.150	-0.373
	Te_{Mo}	-3.69	0.69	1.20	3.48	1.20	2.28	3.36	-0.228	0.154	-0.382
$MoSe_2$	S_{Mo}	-4.22	0.34	0.59	3.49	1.21	2.28	3.67	0.050	0.168	-0.118
	Se_{Mo}	-3.80	0.48	0.84	3.50	1.22	2.28	3.57	0.048	0.184	-0.136
	Te_{Mo}	-3.41	1.04	1.82	3.51	1.24	2.28	3.41	0.053	0.193	-0.140
$MoTe_2$	S_{Mo}	-7.11	13.73	24.42	1.01	-1.72	2.81	2.28	0.752	0.468	0.284
	Se_{Mo}	-4.10	1.35	2.35	2.73	0.47	2.27	2.52	0.621	0.327	0.294
	Te_{Mo}	-3.65	0.45	0.79	2.93	0.69	2.24	2.78	0.578	0.319	0.259
WS_2	S_W	-4.92	18.74	33.92	1.89	-0.64	2.67	2.33	-0.162	0.055	-0.217
	Se_W	-5.91	0.14	0.24	1.17	-1.41	2.58	2.35	-0.040	-0.141	0.101
	Te_W	-3.30	0.28	0.49	3.46	1.19	2.27	3.34	-0.207	0.136	-0.342
WSe_2	S_W	-4.02	0.48	0.85	3.51	1.23	2.28	3.66	0.067	0.156	-0.089
	Se_W	-3.57	0.16	0.28	3.51	1.23	2.28	3.55	0.064	0.215	-0.152
	Te_W	-3.19	1.99	3.47	3.60	1.33	2.27	3.37	0.068	0.142	-0.075
WTe_2	S_W	-6.94	18.03	32.55	0.81	-1.86	2.80	2.27	0.794	0.502	0.292
	Se_W	-3.94	1.07	1.87	2.78	0.53	2.25	2.55	0.601	0.343	0.258
	Te_W	-3.92	5.37	9.40	3.13	0.87	2.27	2.74	0.594	0.259	0.335
MoSSe(↑)	S_{Mo}	-3.86	0.50	0.87	3.39	1.14	2.25	3.51	-0.228	0.132	-0.350
	Se_{Mo}	-4.04	0.29	0.51	3.84	1.16	2.27	3.39	-0.228	0.113	-0.341
	Te_{Mo}	-3.54	0.06	0.11	3.46	1.19	2.27	3.24	-0.230	0.133	-0.363
MoSSe(↓)	S_{Mo}	-3.96	0.23	0.40	3.62	1.33	2.29	3.74	0.076	0.142	-0.065
	Se_{Mo}	-4.17	0.91	1.59	3.37	1.33	2.29	3.68	0.076	0.145	-0.068
	Te_{Mo}	-3.79	0.32	0.56	3.62	1.33	2.29	3.58	0.076	0.135	-0.058
MoSTe(↑)	S_{Mo}	-8.66	89.99	> 5e5	-0.07	-0.07	2.56	2.32	-0.189	-0.086	-0.102
	Se_{Mo}	-3.62	7.67	13.48	3.06	0.78	2.29	2.42	-0.251	0.060	-0.310
	Te_{Mo}	-2.99	5.47	9.58	3.20	0.97	2.24	2.73	-0.196	0.123	-0.319
MoSTe(↓)	S_{Mo}	-6.00	0.54	0.95	1.45	-1.28	2.73	2.23	0.753	0.465	0.289
	Se_{Mo}	-6.07	0.30	0.52	1.41	-1.33	2.74	2.35	0.901	0.491	0.410

	Te_{Mo}	-3.90	0.07	0.12	3.75	1.49	2.26	3.39	0.472	0.165	0.306
MoSeTe(↑)	S_{Mo}	-8.95	73.85	345.28	1.26	-0.30	2.51	2.26	0.403	0.208	0.195
	Se_{Mo}	-3.78	4.56	7.97	3.03	0.79	2.25	2.48	0.050	0.156	-0.105
	Te_{Mo}	-3.27	9.80	17.27	3.18	0.95	2.26	2.75	0.146	0.205	-0.059
MoSeTe(↓)	S_{Mo}	-6.23	0.61	1.06	1.37	-1.35	2.72	2.23	0.754	0.472	0.281
	Se_{Mo}	-6.21	0.39	0.68	1.32	-1.41	2.73	2.37	0.799	0.454	0.345
	Te_{Mo}	-3.87	0.07	0.12	3.77	1.46	2.31	3.96	0.467	0.210	0.257
WSSe(↑)	S_W	-4.20	0.33	0.58	3.38	1.13	2.25	3.50	-0.207	0.213	-0.420
	Se_W	-3.67	0.11	0.20	3.40	1.15	2.25	3.39	-0.209	0.138	-0.348
	Te_W	-3.10	0.48	0.83	3.42	1.17	2.26	3.23	-0.207	0.187	-0.394
WSSe(↓)	S_W	-4.19	5.91	10.36	3.41	1.15	2.27	3.16	0.125	0.208	-0.083
	Se_W	-3.75	0.34	0.59	3.59	1.30	2.29	3.64	0.079	0.179	-0.100
	Te_W	-3.35	0.52	0.91	3.58	1.29	2.28	3.51	0.081	0.161	-0.080
WSTe(↑)	S_W	-5.77	47.38	108.67	2.14	0.56	2.34	2.27	-0.316	-0.036	-0.281
	Se_W	-4.02	8.25	14.51	3.02	0.75	2.29	2.40	-0.210	0.094	-0.305
	Te_W	-2.71	0.31	0.55	3.36	1.14	2.23	2.97	-0.188	0.141	-0.330
WSTe(↓)	S_W	-6.99	13.22	23.50	1.09	-1.77	2.94	2.25	0.723	0.528	0.195
	Se_W	-3.80	0.72	1.25	3.74	1.47	2.26	4.06	0.493	0.194	0.299
	Te_W	-3.74	0.27	0.46	3.73	1.47	2.26	3.96	0.484	0.182	0.303
WSeTe(↑)	S_W	-6.12	51.63	126.29	1.28	-0.28	2.51	2.26	0.160	0.028	0.132
	Se_W	-3.48	0.09	0.15	2.93	1.15	2.22	2.74	0.082	0.161	-0.079
	Te_W	-3.25	9.66	17.02	3.14	1.17	2.26	2.73	0.156	0.201	-0.046
WSeTe(↓)	S_W	-4.33	9.02	15.87	3.43	1.17	2.29	3.30	0.575	0.250	0.324
	Se_W	-3.97	0.02	0.04	3.65	1.30	2.25	3.97	0.474	0.198	0.276
	Te_W	-3.74	0.15	0.26	3.65	1.29	2.28	3.78	0.482	0.224	0.258

S6. Optimized configurations of Ir_2@TMD-X_M nanosheets.

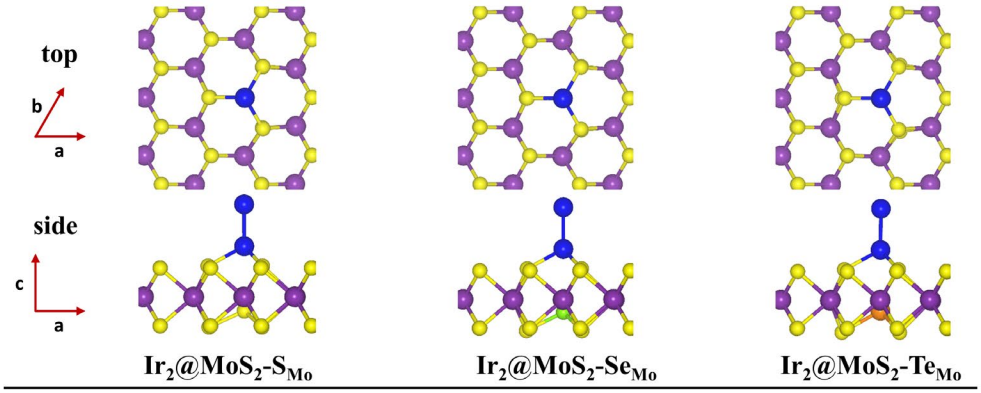

Ir_2@MoS_2-S_{Mo} | Ir_2@MoS_2-Se_{Mo} | Ir_2@MoS_2-Te_{Mo}

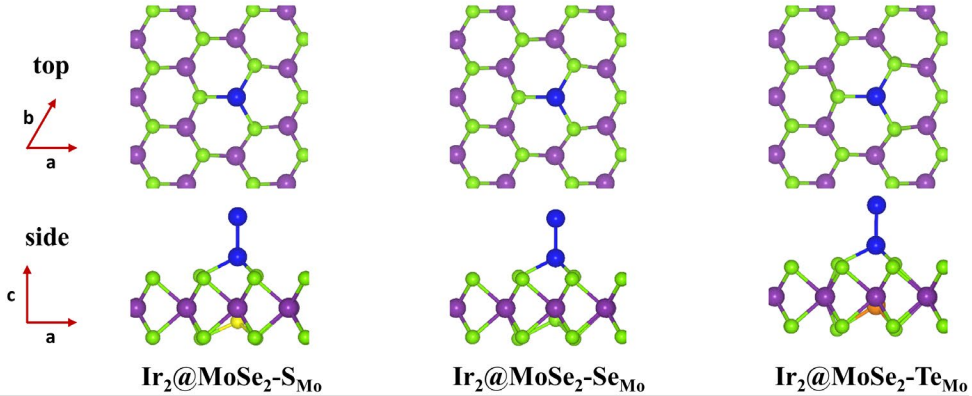

Ir_2@$MoSe_2$-S_{Mo} | Ir_2@$MoSe_2$-Se_{Mo} | Ir_2@$MoSe_2$-Te_{Mo}

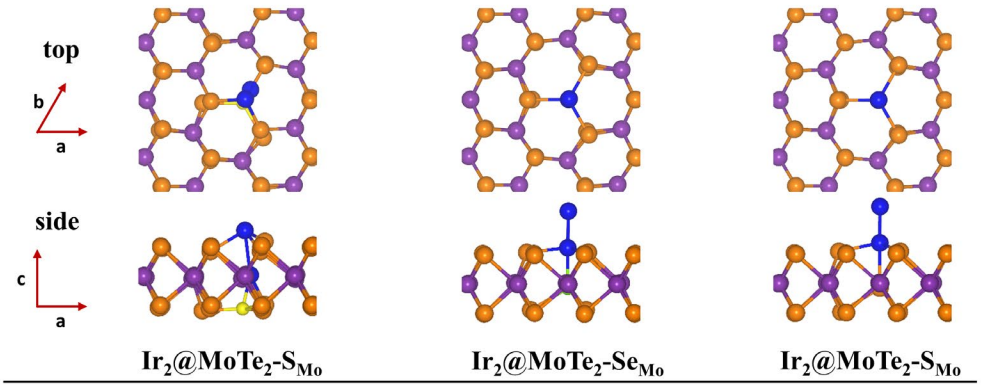

Ir_2@$MoTe_2$-S_{Mo} | Ir_2@$MoTe_2$-Se_{Mo} | Ir_2@$MoTe_2$-S_{Mo}

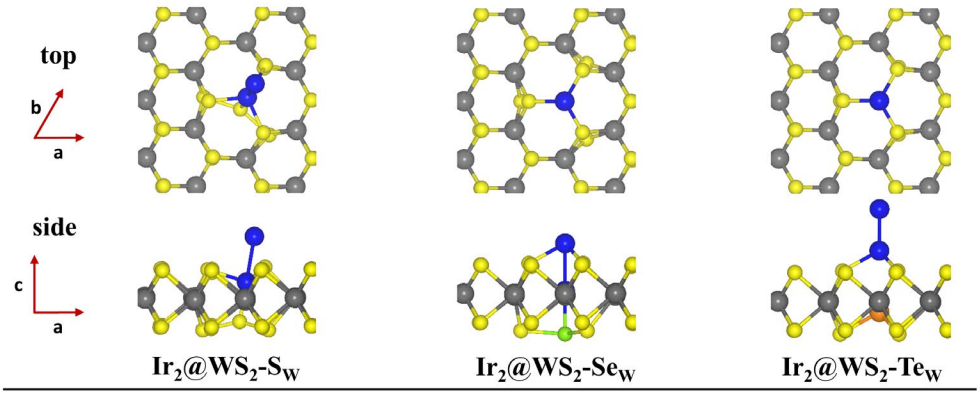

Ir_2@WS_2-S_W | Ir_2@WS_2-Se_W | Ir_2@WS_2-Te_W

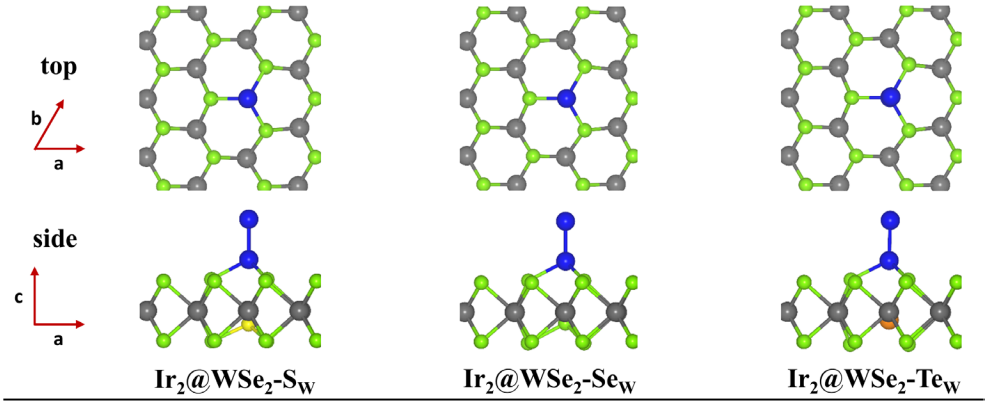

$Ir_2@WSe_2$-S_W | $Ir_2@WSe_2$-Se_W | $Ir_2@WSe_2$-Te_W

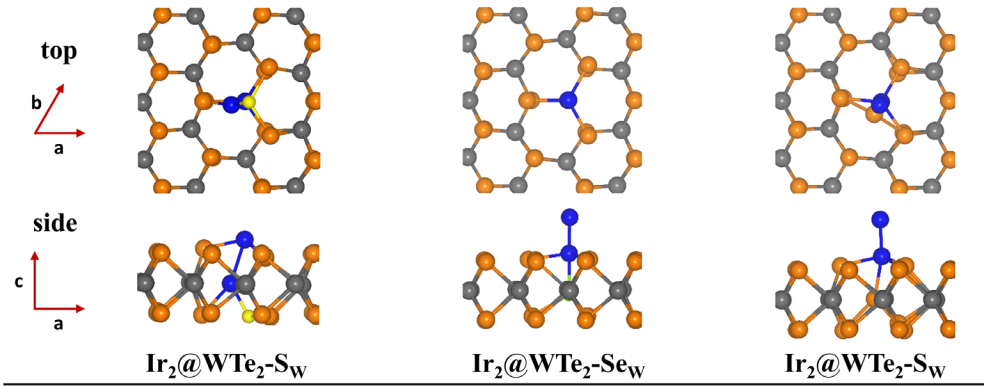

$Ir_2@WTe_2$-S_W | $Ir_2@WTe_2$-Se_W | $Ir_2@WTe_2$-S_W

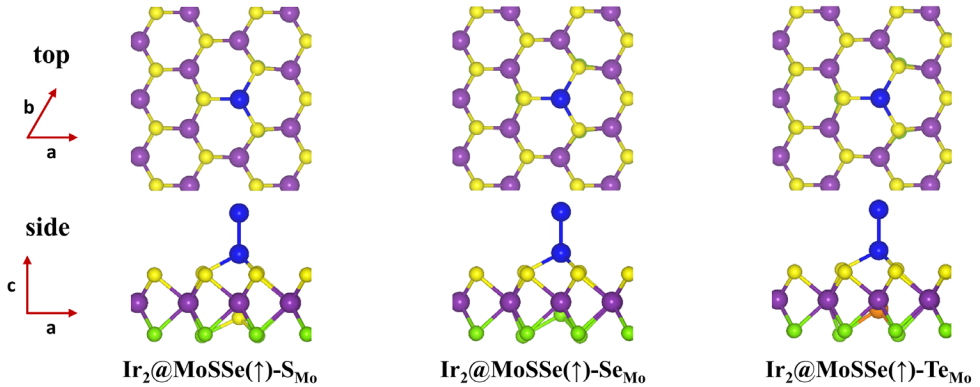

$Ir_2@MoSSe(\uparrow)$-S_{Mo} | $Ir_2@MoSSe(\uparrow)$-Se_{Mo} | $Ir_2@MoSSe(\uparrow)$-Te_{Mo}

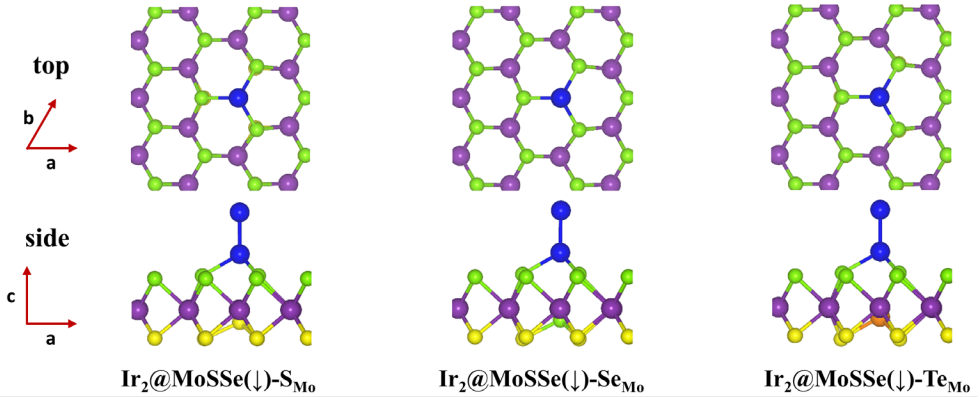

$Ir_2@MoSSe(\downarrow)$-S_{Mo} | $Ir_2@MoSSe(\downarrow)$-Se_{Mo} | $Ir_2@MoSSe(\downarrow)$-Te_{Mo}

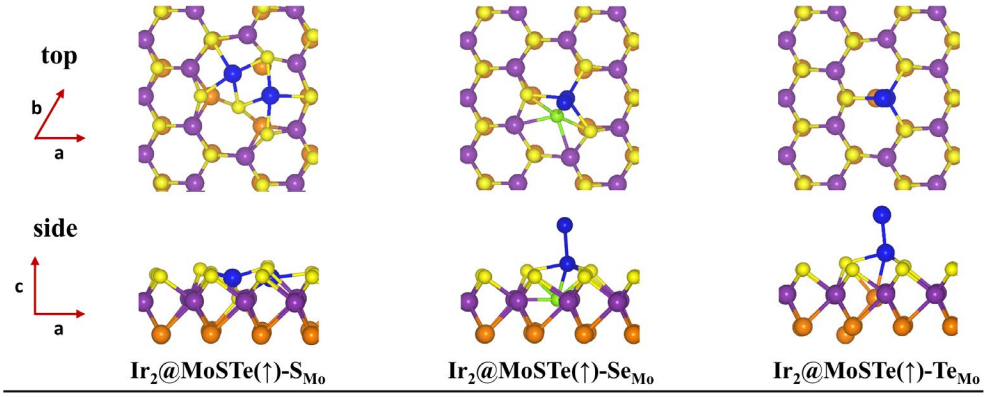

Ir_2@MoSTe(↑)-S_{Mo} | Ir_2@MoSTe(↑)-Se_{Mo} | Ir_2@MoSTe(↑)-Te_{Mo}

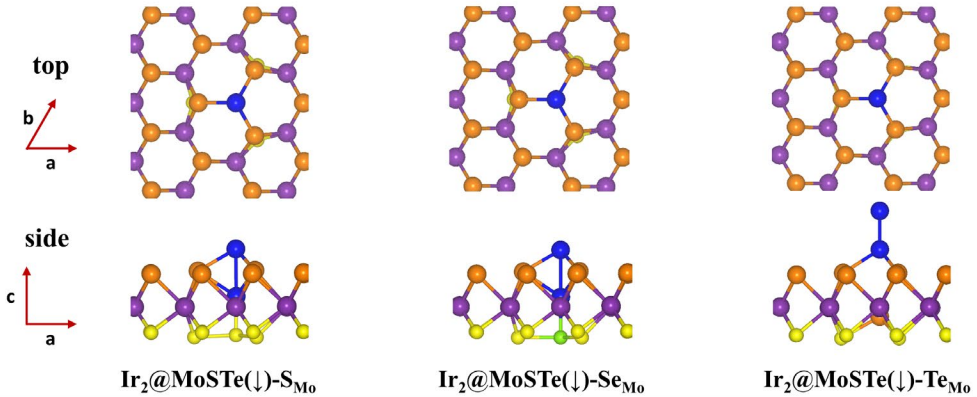

Ir_2@MoSTe(↓)-S_{Mo} | Ir_2@MoSTe(↓)-Se_{Mo} | Ir_2@MoSTe(↓)-Te_{Mo}

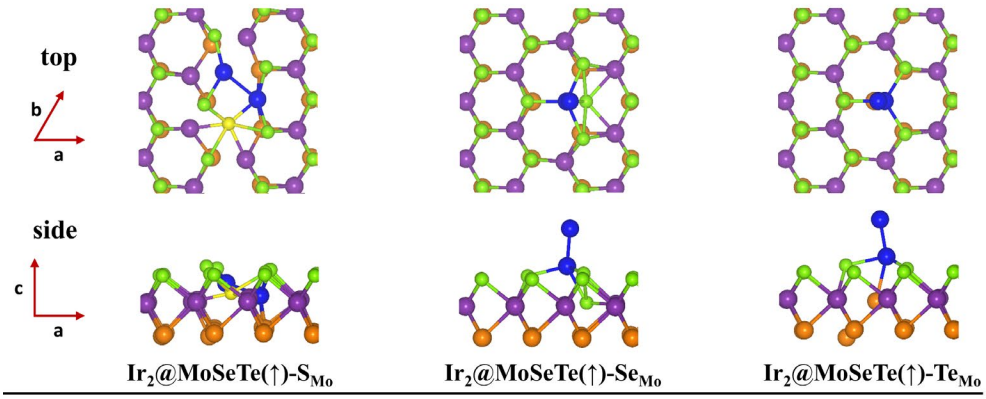

Ir_2@MoSeTe(↑)-S_{Mo} | Ir_2@MoSeTe(↑)-Se_{Mo} | Ir_2@MoSeTe(↑)-Te_{Mo}

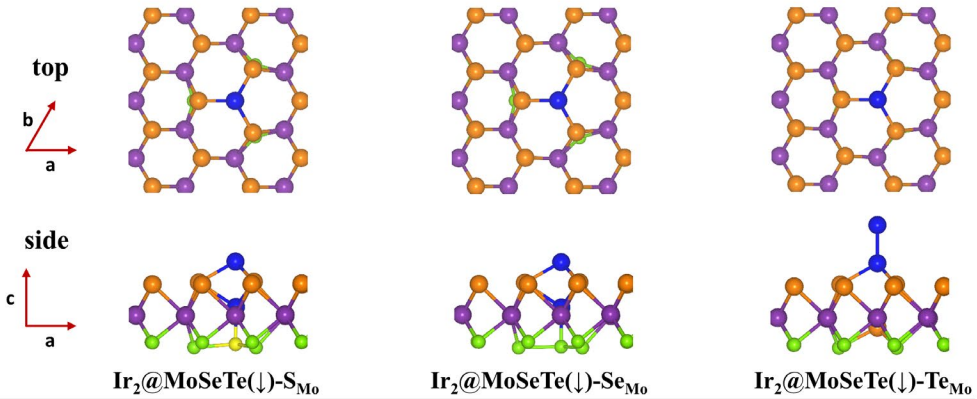

Ir_2@MoSeTe(↓)-S_{Mo} | Ir_2@MoSeTe(↓)-Se_{Mo} | Ir_2@MoSeTe(↓)-Te_{Mo}

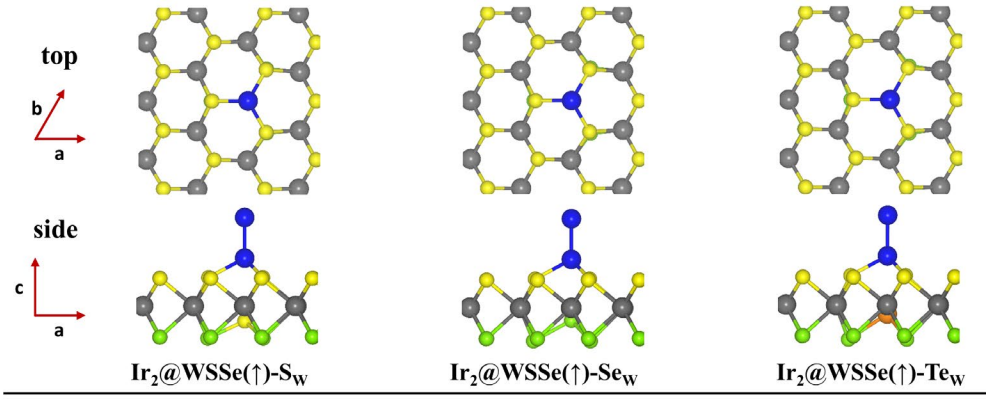

Ir_2@WSSe(↑)-S_W | Ir_2@WSSe(↑)-Se_W | Ir_2@WSSe(↑)-Te_W

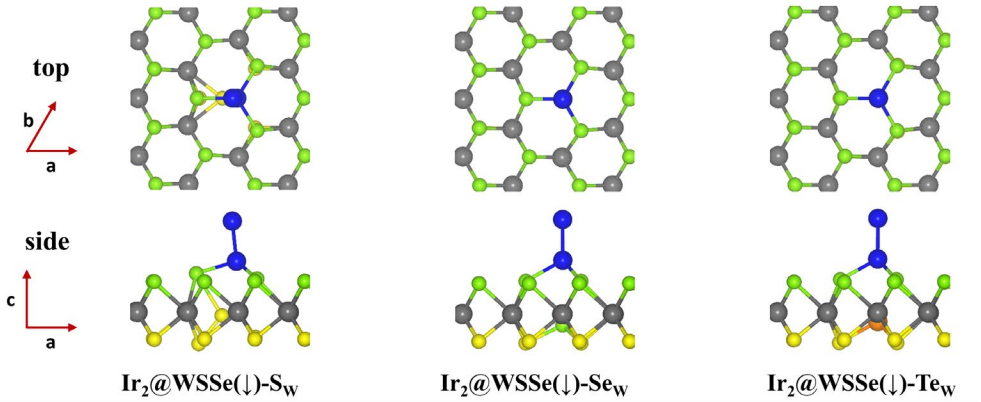

Ir_2@WSSe(↓)-S_W | Ir_2@WSSe(↓)-Se_W | Ir_2@WSSe(↓)-Te_W

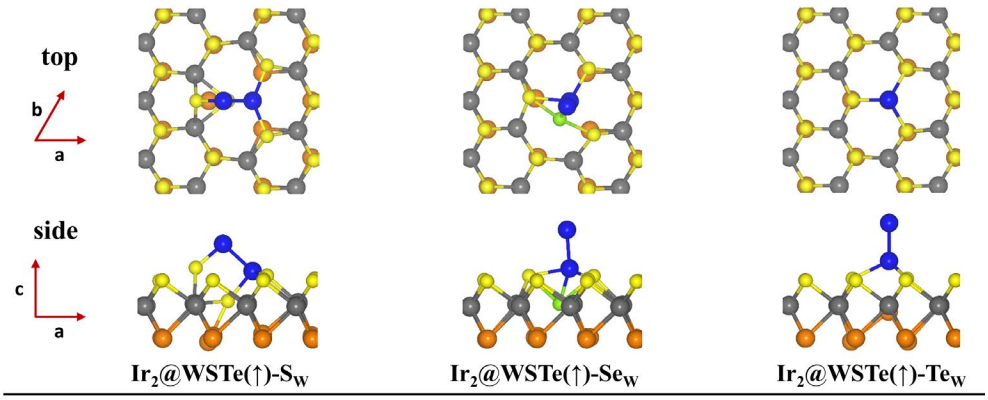

Ir_2@WSTe(↑)-S_W | Ir_2@WSTe(↑)-Se_W | Ir_2@WSTe(↑)-Te_W

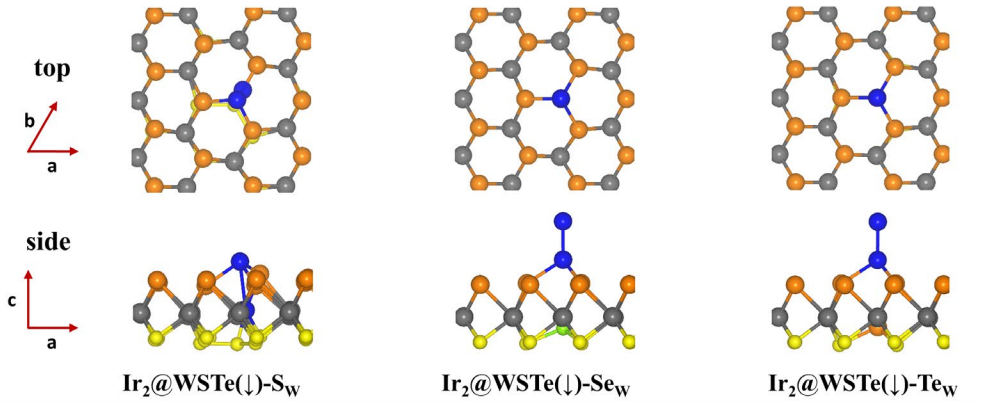

Ir_2@WSTe(↓)-S_W | Ir_2@WSTe(↓)-Se_W | Ir_2@WSTe(↓)-Te_W

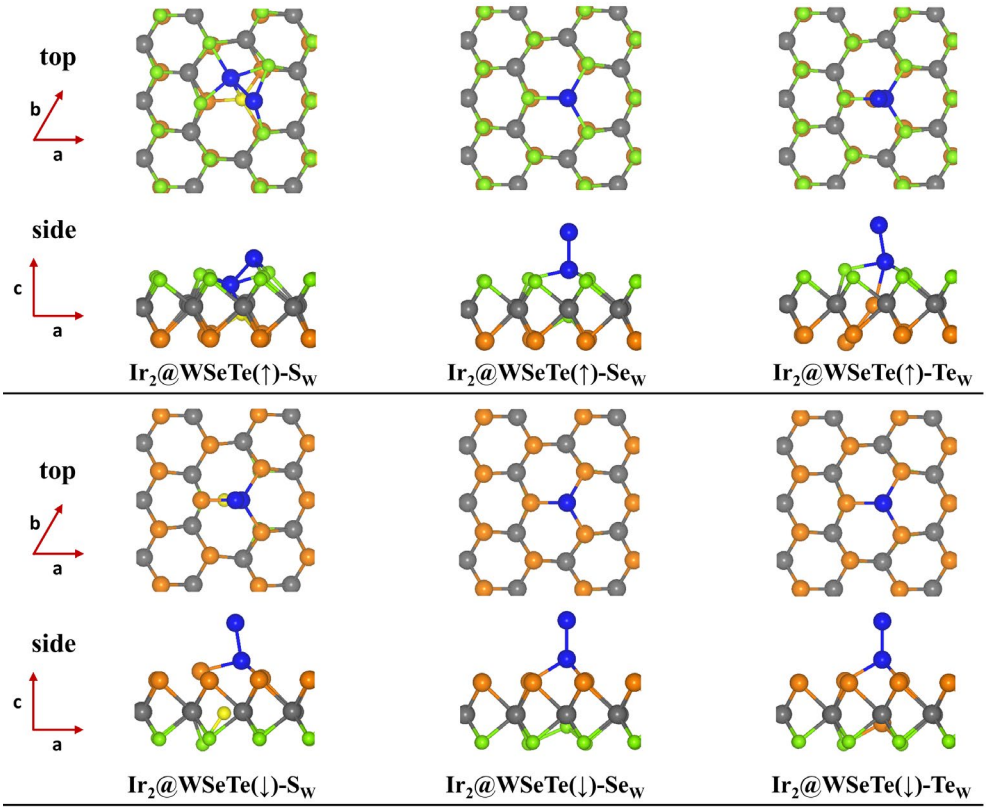

Fig. S3 Top and side views of Ir_2@TMD-X_M (M = Mo, W; X = S, Se, Te) nanosheets. The yellow, green, orange, purple, grey and blue balls represent S, Se, Te, Mo, W and Ir atoms, respectively.

S7. The dissociation energy of top Ir atom and Ir_2 from Ir_2@TMD-X_M configurations.

In order to further verify the stability of the composite structures, the dissociation energies $E_d(Ir_2)$ and $E_d(Ir^A)$ are plotted in Figure S3, using the following formula:

$$E_d = E_{Ir^A/Ir_2} + E_{re} - E_{Ir_2@TMD\text{-}X_M}$$

where $E_{Ir_2@TMD\text{-}X_M}$, E_{Ir^A/Ir_2} and E_{re} are the energies of the adsorbed Ir_2 dimer TMD systems, freestanding Ir^A atom or Ir_2 dimer, the remain part after dissociating, respectively.

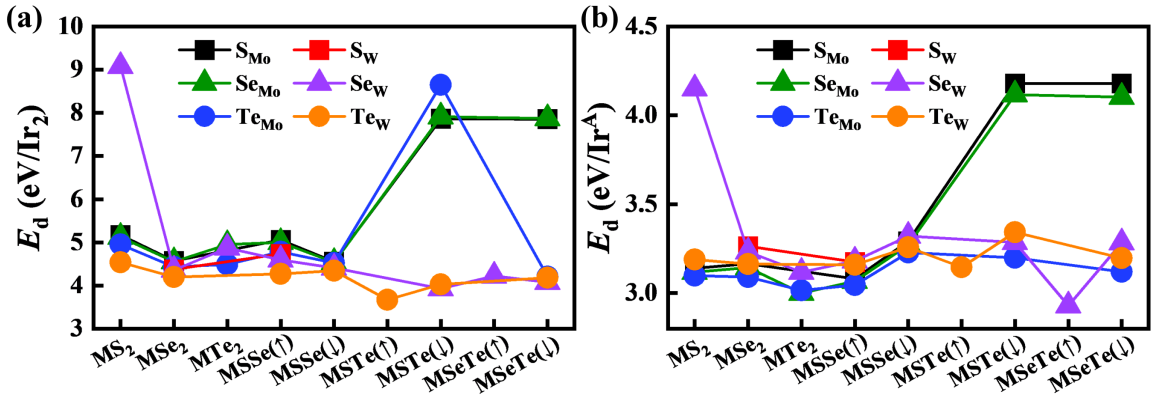

Fig. S4 The dissociation energy E_d for (c) Ir_2 dimer and (d) top Ir^A atom dissociating from composite systems. Here M (= Mo, W) in the abscissa is the same as M of X_M in legend.

S8. Magnetic parameters of vertical Ir_2@TMD-X_M nanosheets.

Table S4. MAEs (meV), total magnetic moments M (μ_B), spin moments M_S(μ_B) and orbital moments M_L (μ_B) of 37 vertical Ir_2@TMD-X_M structures.

TMDs	Defect	MAE	M_{tot}	$M(Ir_2)$	Ir^A				Ir^B			
					$M_S^{\parallel}$	$M_S^{\perp}$	$M_L^{\parallel}$	$M_L^{\perp}$	$M_S^{\parallel}$	$M_S^{\perp}$	$M_L^{\parallel}$	$M_L^{\perp}$
MoS_2	S_{Mo}	71.09	1.644	1.603	0.953	0.039	0.336	1.400	0.209	0.268	0.073	0.017
	Se_{Mo}	70.33	1.672	1.639	0.903	0.060	0.347	1.388	0.211	0.273	0.077	0.017
	Te_{Mo}	70.83	1.695	1.673	0.920	0.082	0.343	1.375	0.219	0.278	0.074	0.018
$MoSe_2$	S_{Mo}	70.71	1.741	1.724	0.918	0.097	0.348	1.354	0.235	0.295	0.097	0.035
	Se_{Mo}	69.33	1.762	1.761	0.932	0.120	0.351	1.344	0.241	0.303	0.097	0.035
	Te_{Mo}	70.71	1.764	1.783	0.950	0.139	0.342	1.335	0.243	0.307	0.099	0.034
$MoTe_2$	Se_{Mo}	-3.64	0.078	0.173	0.229	-0.083	0.019	0.297	-0.026	0.006	-0.001	-0.047
	Te_{Mo}	-1.90	-0.033	-0.102	-0.150	-0.086	0.020	0.153	0.035	0.020	0.026	0.027
WS_2	Se_W	0	0	0	0	0	0	0	0	0	0	0
	Te_W	75.93	1.698	1.577	0.903	0.021	0.313	1.415	0.215	0.280	0.088	0.025
WSe_2	S_W	70.69	1.702	1.705	0.924	0.072	0.323	1.366	0.235	0.301	0.112	0.045
	Se_W	70.63	1.732	1.749	0.941	0.100	0.326	1.353	0.243	0.309	0.110	0.044
	Te_W	72.61	1.735	1.768	0.958	0.118	0.316	1.346	0.244	0.308	0.109	0.044
WTe_2	Se_W	0.85	-0.025	-0.046	-0.074	-0.004	0.003	-0.037	0.008	-0.002	-0.005	0.010
MoSSe(↑)	S_{Mo}	79.13	1.388	1.371	0.836	-0.070	0.296	1.467	0.196	0.260	0.076	0.016
	Se_{Mo}	74.46	1.553	1.534	0.877	0.010	0.331	1.424	0.199	0.270	0.082	0.014
	Te_{Mo}	73.67	1.636	1.622	0.914	0.060	0.325	1.387	0.213	0.279	0.078	0.015
MoSSe(↓)	S_{Mo}	65.22	1.815	1.783	0.923	0.137	0.378	1.324	0.237	0.277	0.080	0.043
	Se_{Mo}	65.23	1.820	1.800	0.923	0.151	0.389	1.320	0.237	0.281	0.084	0.043
	Te_{Mo}	67.75	1.785	1.779	0.929	0.139	0.378	1.335	0.233	0.279	0.085	0.041
MoSTe(↓)	S_{Mo}	0	0	0	0	0	0	0	0	0	0	0
	Se_{Mo}	0	0	0	0	0	0	0	0	0	0	0
	Te_{Mo}	64.73	1.808	1.842	0.889	0.155	0.465	1.402	0.141	0.135	0.091	-0.004
MoSeTe(↓)	S_{Mo}	0	0	0	0	0	0	0	0	0	0	0
	Se_{Mo}	0	0	0	0	0	0	0	0	0	0	0
	Te_{Mo}	65.88	1.811	1.851	0.947	0.165	0.389	1.330	0.249	0.297	0.103	0.054
WSSe(↑)	S_W	82.01	1.254	1.273	0.823	-0.108	0.286	1.492	0.201	0.273	0.098	0.016
	Se_W	81.35	1.317	1.343	0.838	-0.079	0.279	1.476	0.202	0.275	0.087	0.017
	Te_W	82.14	1.389	1.432	0.872	-0.036	0.280	1.448	0.202	0.276	0.092	0.020
WSSe(↓)	Se_W	67.66	1.801	1.801	0.945	0.133	0.350	1.328	0.246	0.298	0.099	0.047

	Te_W	69.19	1.779	1.796	0.949	0.134	0.346	1.335	0.241	0.298	0.104	0.047
WSTe(↑)	Te_W	79.06	0.917	1.029	0.909	0.083	0.358	1.354	0.239	0.276	0.103	0.067
WSTe(↓)	Se_W	69.68	1.721	1.742	0.717	-0.159	0.186	1.430	0.134	0.258	0.110	-0.012
	Te_W	73.52	1.679	1.724	0.914	0.072	0.356	1.376	0.236	0.275	0.104	0.067
WSeTe(↑)	Se_W	-0.98	-0.043	-0.077	-0.131	0.010	-0.023	0.038	0.023	0.041	0.019	0.027
WSeTe(↓)	Se_W	71.09	1.688	1.709	0.918	0.056	0.321	1.367	0.241	0.284	0.114	0.072
	Te_W	68.72	1.780	1.829	0.959	0.139	0.354	1.343	0.239	0.293	0.118	0.062

S9. Projected density of states of Ir_2@TMD-X_M nanosheets.

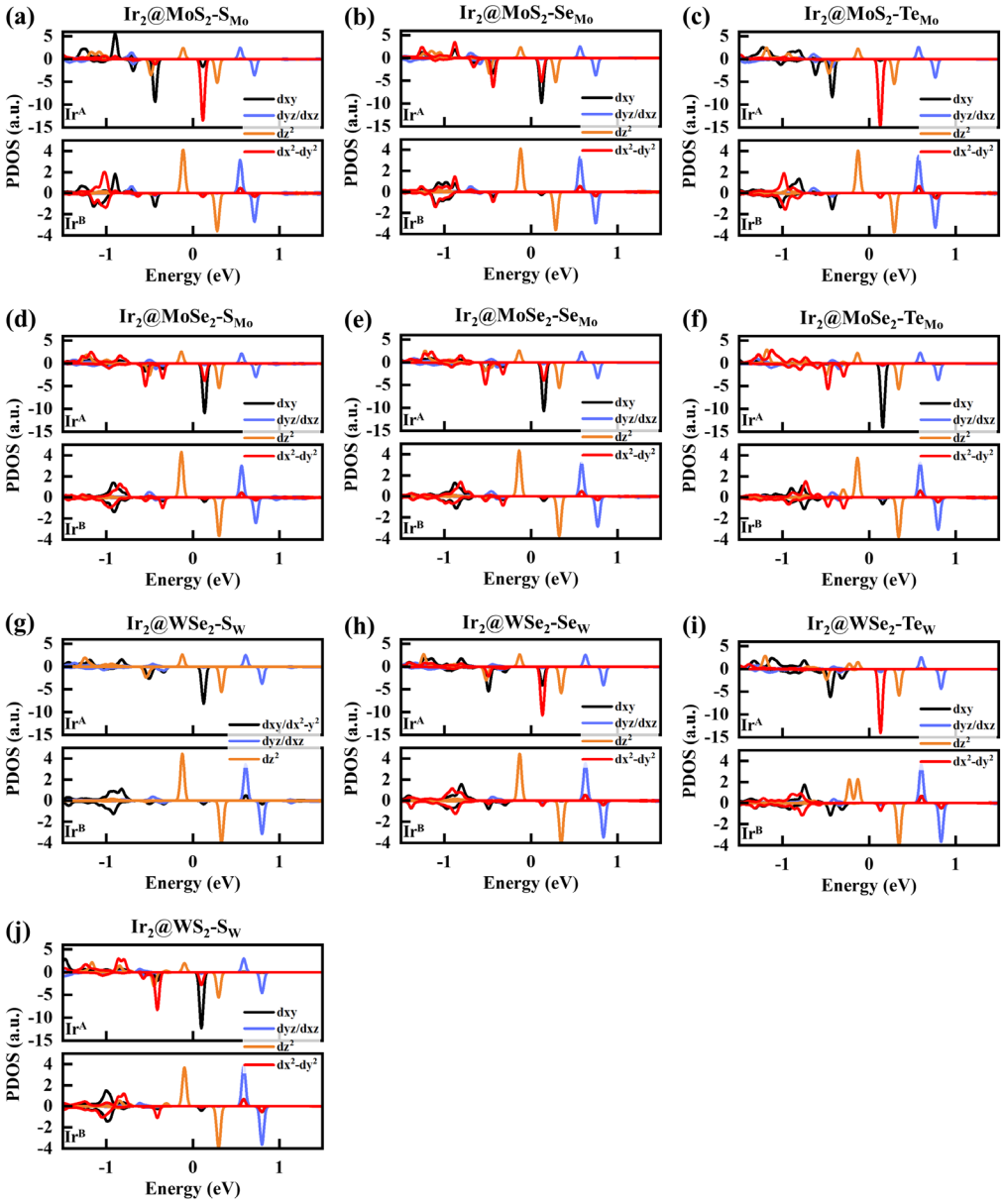

Fig. S5 Projected density of states of d orbitals of Ir^A and Ir^B atoms in Ir_2@MX_2-X_M (M = Mo, W; X = S, Se, Te) structures.

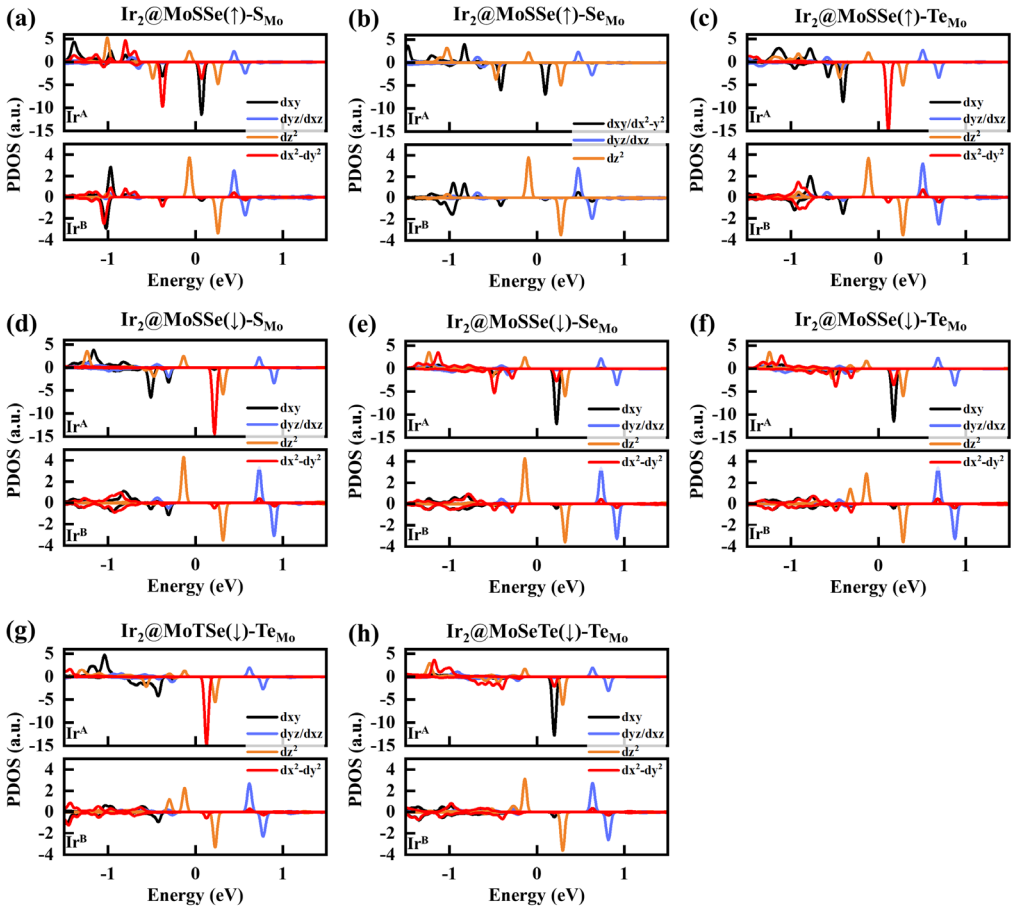

Fig. S6 Projected density of states of d orbitals of Ir^A and Ir^B atoms in Ir_2@MoXY-X_{Mo} (X, Y = S, Se, Te; X≠Y) structures.

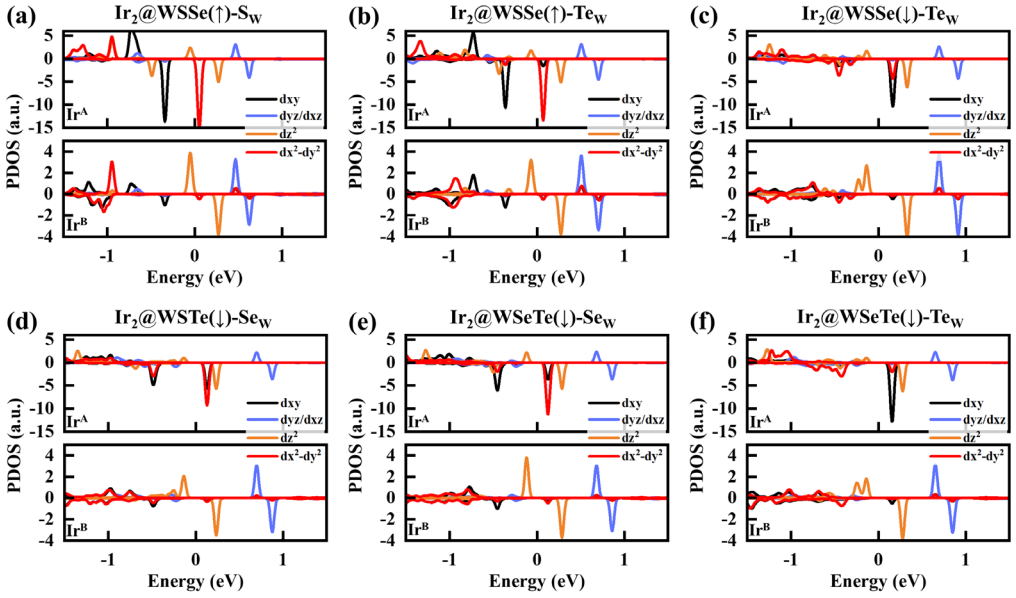

Fig. S7 Projected density of states of d orbitals of Ir^A and Ir^B atoms in Ir_2@WXY-X_W (X, Y = S, Se, Te; X≠Y) structures.

S10. The d-orbital resolved MAE of Ir atoms in Ir_2@TMD-X_M nanosheets.

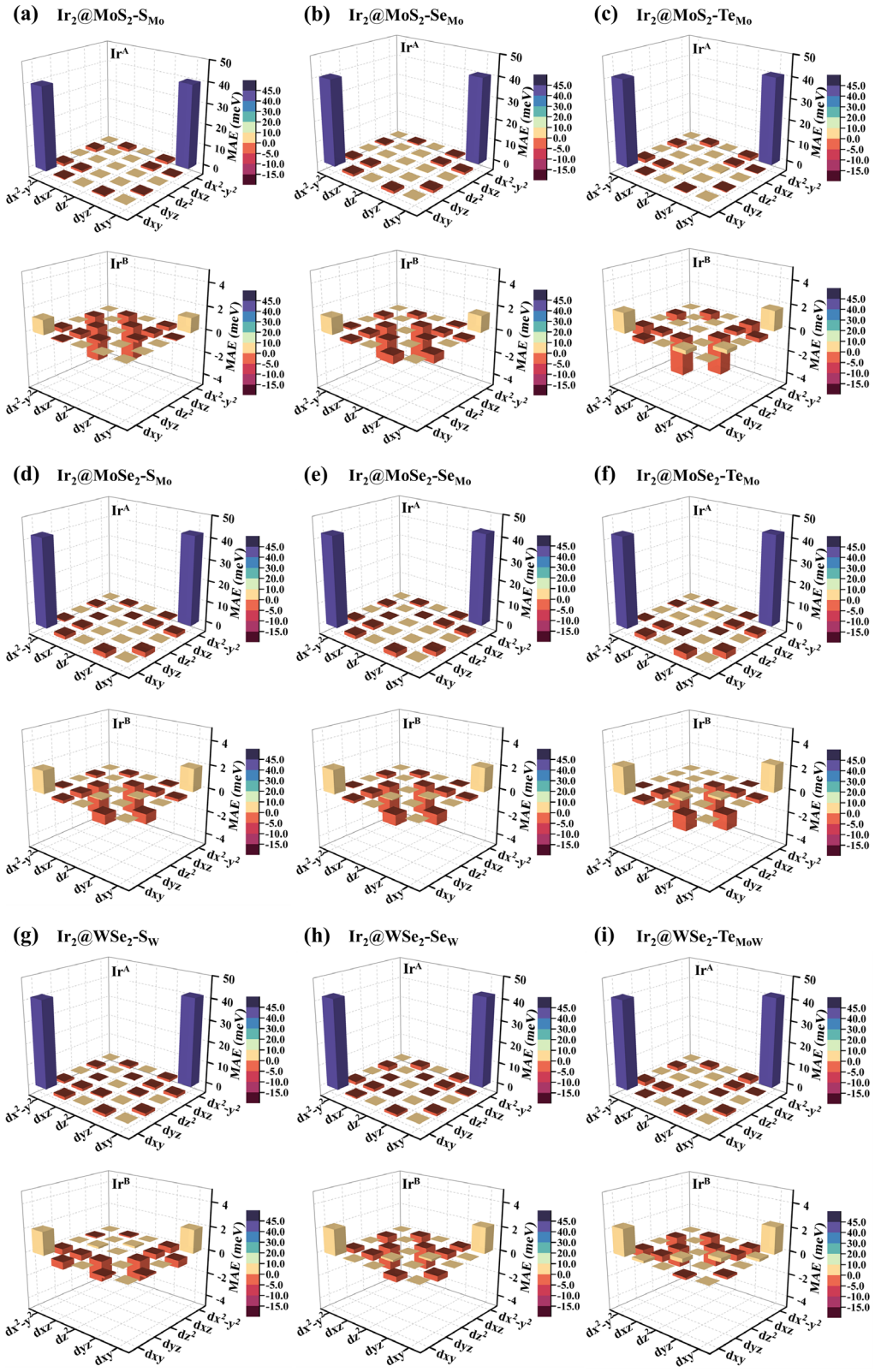

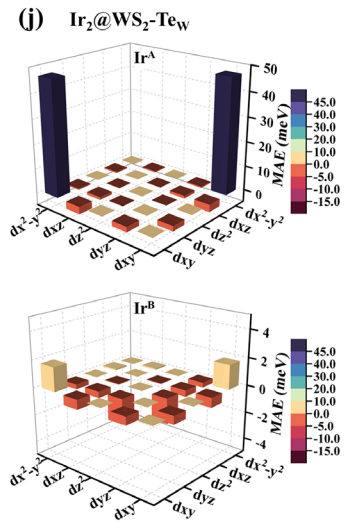

Fig. S8 The d-orbital resolved MAE of Ir^A and Ir^B atoms in $Ir_2@MX_2$-X_M (M = Mo, W; X = S, Se, Te) structures.

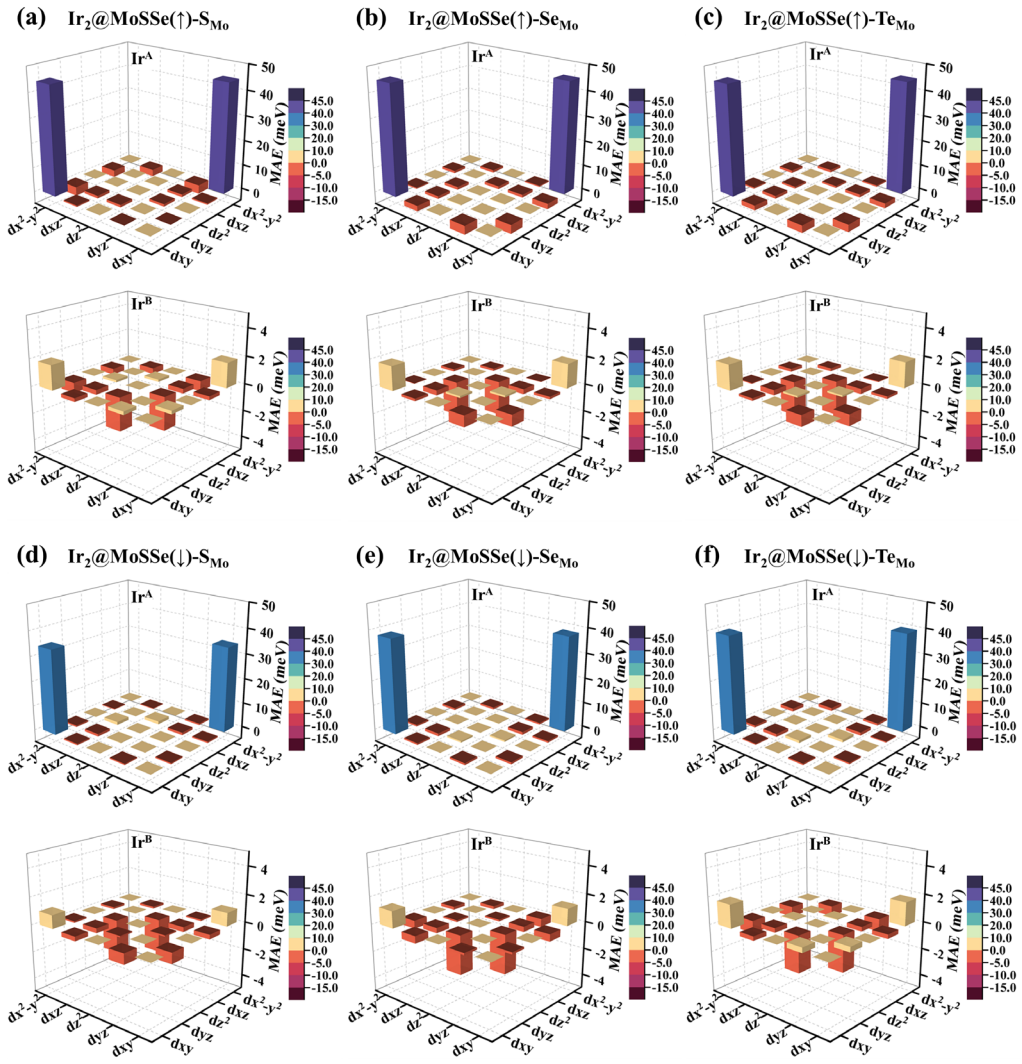

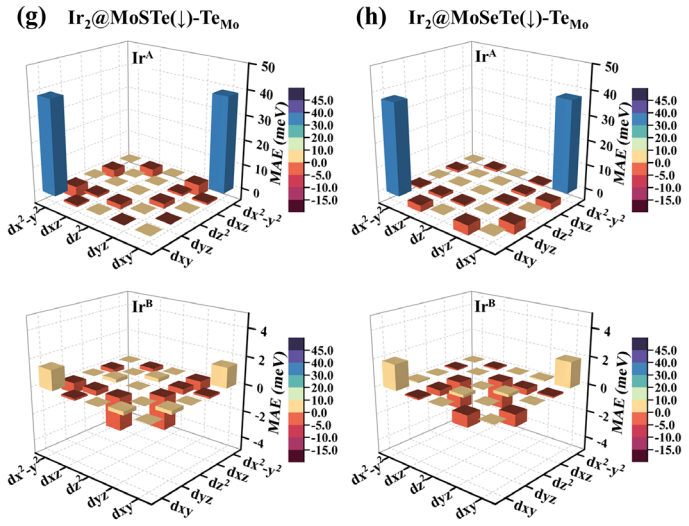

Fig. S9 The d-orbital resolved MAE of Ir^A and Ir^B atoms in Ir_2@MoXY-X_{Mo} (X, Y = S, Se, Te; X≠Y) structures.

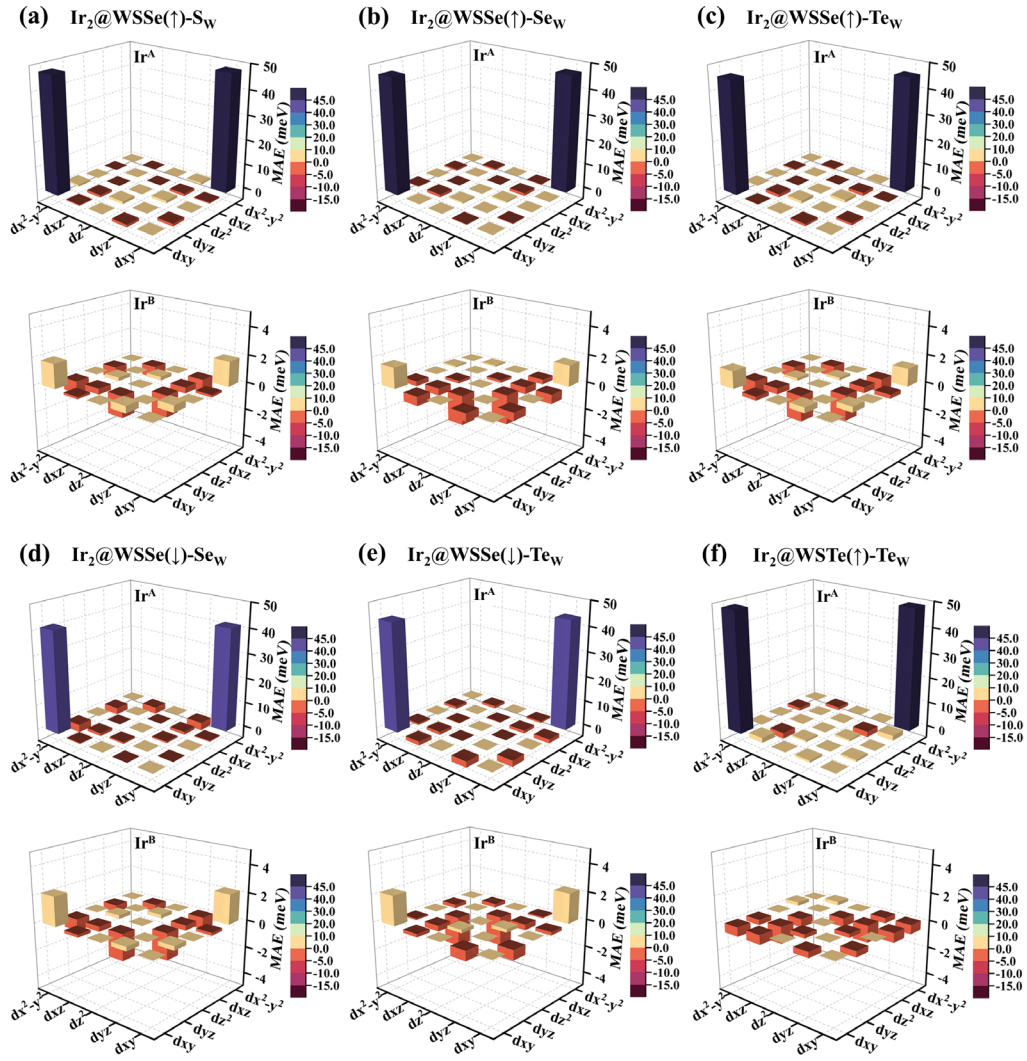

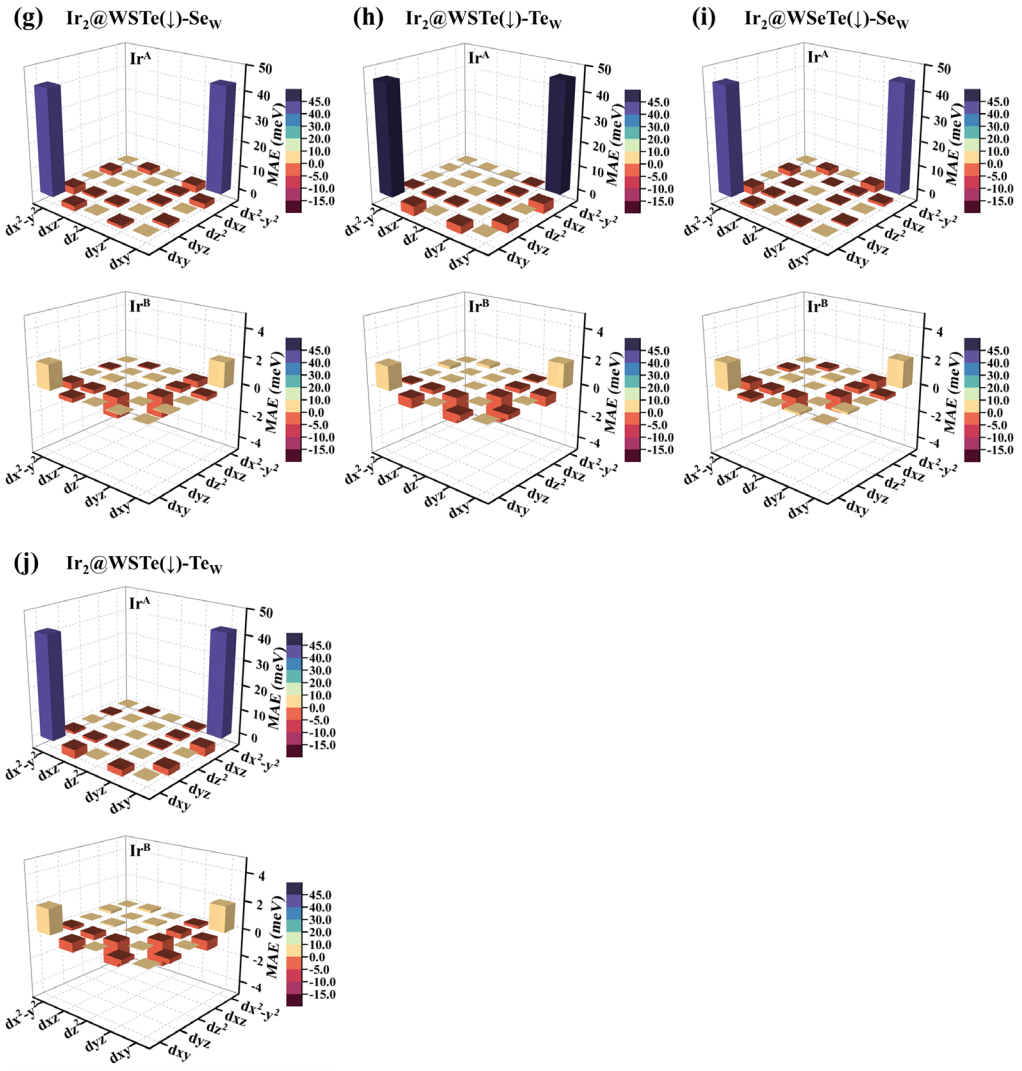

Fig. S10 The d-orbital resolved MAE of Ir^A and Ir^B atoms in Ir_2@WXY-X_W (X, Y = S, Se, Te; X≠Y) structures.

S11. The relationship among ΔV, ε_{dd}, ε_{ud} of vertical Ir_2 above TMD-X_M nanosheets.

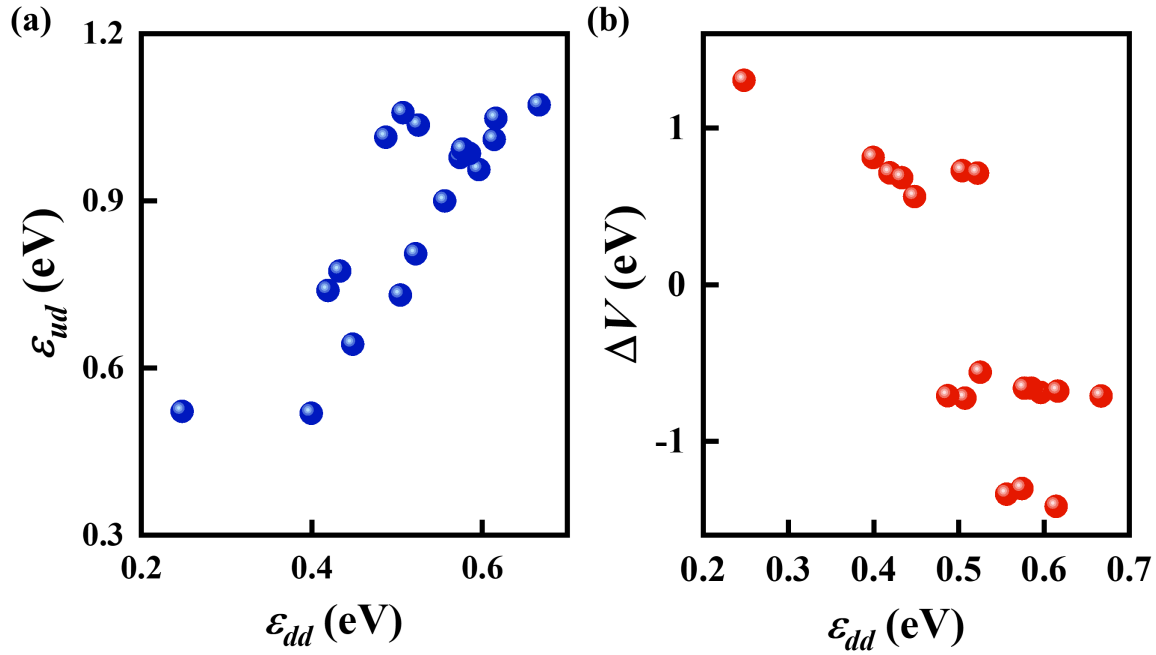

Fig. S11 (a) The energy eigenvalues difference between occupied and unoccupied states in cross-spin spin states ε_{ud} as a function of the one in minority states ε_{dd}. (b) The average electrostatic potential differences ΔV (eV) as a function of energy eigenvalues difference between occupied and unoccupied states ε_{dd} in minority spin states.

S12. The values of ε_{dd} and ε_{ud} of vertical Ir_2 above Janus TMD-X_M nanosheets.

Table S5. Energy differences ε_{dd} and ε_{ud} of Ir_2@ Janus TMD-X_M monolayers with large MAEs (> 60 mev/Ir_2).

Substrates	ε_{dd} (eV)			ε_{ud} (eV)		
	S_M	Se_M	Te_M	S_M	Se_M	Te_M
MoSSe(↑)	0.448	0.504	0.522	0.643	0.731	0.805
MoSSe(↓)	0.525	0.507	0.487	1.036	1.058	1.014
MoSTe(↑)	-	-	-	-	-	-
MoSTe(↓)	-	-	0.556	-	-	0.900
MoSeTe(↑)	-	-	-	-	-	-
MoSeTe(↓)	-	-	0.596	-	-	0.956
WSSe(↑)	0.399	0.419	0.433	0.519	0.739	0.774
WSSe(↓)	-	0.667	0.616	-	1.072	1.048
WSTe(↑)	-	-	0.248	-	-	0.522
WSTe(↓)	-	0.614	0.574	-	1.010	0.978
WSeTe(↑)	-	-	-	-	-	-
WSeTe(↓)	-	0.585	0.577	-	0.985	0.993